

Experimental study on micro diffusion flame of liquid fuels from a micro tube

Junwei Li, Zuozen Qiu, Rong Yao, Ningfei Wang

School of Aerospace Engineering, Beijing Institute of Technology,

Beijing 100081, PR China

1 Introduction

Micro power systems with hydrocarbon fuel have energy density about 100 times higher than that of the most advanced batteries. In the past few years, much attentions have been paid on these systems. To make micro-combustors steadily operate, a micro-jet flame may be used as a point heat source or utilized for power generation. Therefore, an understanding of the physics and chemistry of the laminar micro-jet flame is of vital importance^[1]. But compared with gaseous fuels, there were few researches about micro jet flame using liquid fuels. In this study, we investigate the influence of n-heptane flow rates, fuel types and tube materials on the characteristics of the micro diffusion flame of liquid fuels. The micro diffusion flame is stabilized on a micro quartz tube with inner diameter of 0.2mm. The fuel flow rate and fuel types in the micro tube could be varied, and the quartz and stainless steel tubes are used to vary the tube materials. The stability limit, flame size and shape are examined experimentally, and the stabilization mechanism is discussed based on those results.

2 Experimental setup

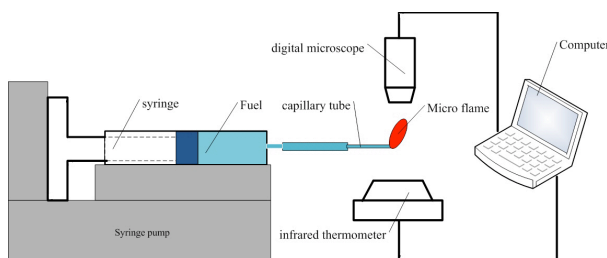


Fig. 1 Schematic of the experimental setup

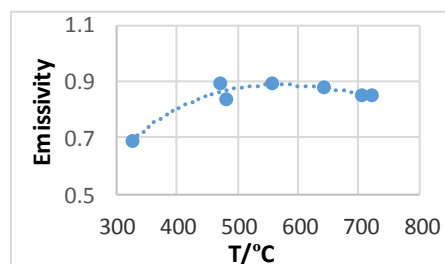


Fig. 2 Emissivity vs. wall temperature

The experimental apparatus, as shown in Fig. 1, consists of a micro tube, fuel supplying system, observation system, and temperature measurement system. In experiments, the micro tube is installed horizontally on a syringe. Two types of tube are chosen to supply liquid fuel, which are quartz and stainless steel tubes with outer diameter of 0.5mm and inner diameter of 0.2mm. A syringe pump (LSP01-1A) and a plastic syringe with inner diameter of 10 mm are used to supply liquid fuels into the

tube and a small diffusion flame is stabilized at the tube exit. All experiments were conducted at room temperature and one atmosphere.

The fuel flow rate is accurately controlled by the syringe pump with an error of less than 1.0%. The micro flame observation system is composed of a stereo microscope (three million pixels), a digital camera (MT9V032, 752×480 pixels, Qimeng optics, Shenzhen, China), and an observing computer. The micro flame is captured by the camera at a frame rate of 128 fps. An infrared radiation (IR) camera (FLIR, A40) of a temperature range of 0-1500°C is used to measure surface temperature of the capillary tube. Field view of the IR camera is 64mm×48mm, which is fitted with 150mm macro lens. The measured spectral range is 7.5 to 13μm. The IR images are used to illustrate the temperature differences on the tube surface. A software (FLIR Report) is used to measure wall temperature of the tube with an error of less than ±2°C. Calibration of the thermography imaging camera was conducted. The calibrated emissivity of the quartz tube is shown in Fig.2. The values of emissivity for micro quartz tube and stainless steel tube are both taken as 0.85 in this study.

3 Results and discussion

3.1 Combustion characteristics of n-heptane

In a static environment, a micro diffusion flame is affected by the fuel flow rate. Its length and shape are influenced by the flow rate due to using liquid fuel. In the experiments, n-heptane is used as liquid fuel and the flow rate changes from 5 μl/min to 70 μl/min. For convenience, a micro quartz tube is used to observe the flame and gas-liquid interface.

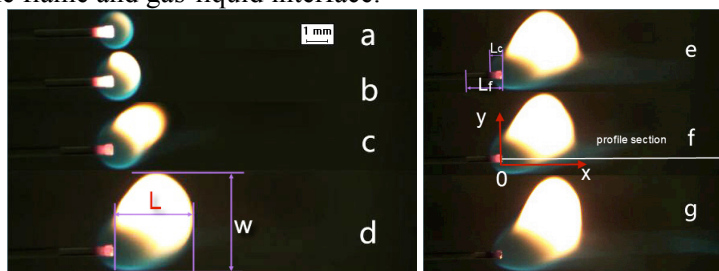


Fig. 3 Flame photos of n-heptane at different fuel flow rate (Q_f). (a) 5 μl/min, (b) 10 μl/min, (c) 20 μl/min, (d) 30 μl/min, (e) 40 μl/min, (f) 50 μl/min, (g) 70 μl/min

As shown in Fig. 3(a) and (b), when $Q_f \leq 10$ μl/min, the flame is very short, no larger than 1mm and its shape is like a ball, due to less affected by the buoyancy force. In these figures, it can be seen that there are two colors in the flame, the upper part emitting yellow light and the lower part emitting blue light. Yellow light of the flame is emitted by soot particles and blue light results from excited CH radicals. Therefore, it can be concluded that main reaction occurs at the tube exit. In addition, we can also see that the wall near the tube tip is heated to white, indicating the wall being very hot. Furthermore, as seen in Fig. 3(c)-(f), when $Q_f \geq 20$ μl/min, the flame does not look like a ball, and it is stretched longer. In the upper right region of the flame, bright yellow light is emitted. While at the downstream region of the tip, a dark blue plume still exists, which is not affected by the flow rates. With increasing of fuel flow rate, the tube wall at the end gradually darkens from red to black due to the flame being far from the tube exit. At $Q_f = 70$ μl/min, Fig. 3(f) shows that the flame length do not change much and there is some blue plume ejected from the tube. This is the flame covering unevaporated droplets ejected from the tube due to larger flow rate and low wall temperature.

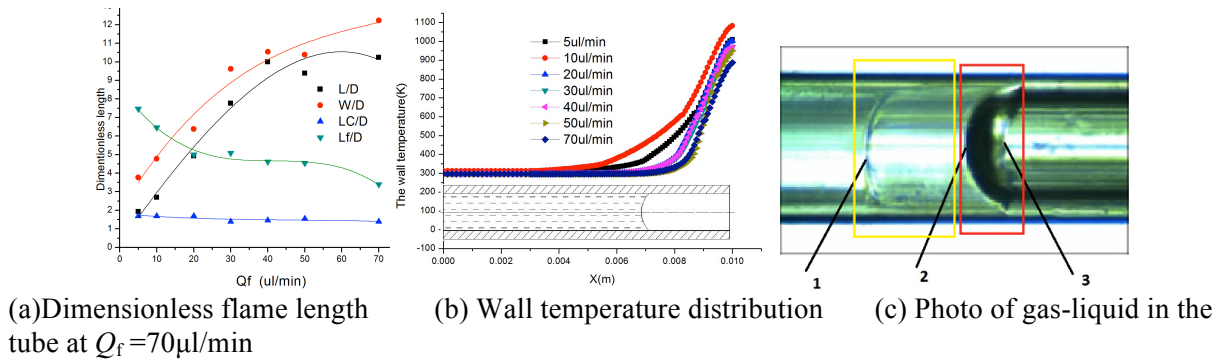


Fig. 4 Flame characteristics of n-heptane

Fig. 4(a) shows that when $Q_f = 5 \mu\text{l/min}$, L/D is only 2, and W/D is 4. The flame is like a bright blue ball, which is affected little by the buoyancy force. The gas-liquid interface is 2.54mm from the tube exit. When $Q_f > 40 \mu\text{l/min}$, the flame width (W/D) increases with increasing of flow rate, but the flame length (L/D) is almost unchanged. When Q_f is up to $70 \mu\text{l/min}$, the jet flame becomes unstable, jumping and accompanied by a whirring sound and reaches the longest, 6.07mm. The flame is greatly affected by the buoyancy force. Before combustion of liquid fuel, the liquid fuel must be vaporized. Therefore there is a gas-liquid interface in the tube, which is affected by wall temperature of the tube. In Fig. 4(b), we can see that the distance between the interface and the tube exit (L_f/D) decreases with increasing of the fuel flow rate, and the interface moves to the capillary exit. When $Q_f = 5 \mu\text{l/min}$, L_f/D is up to 7.5. But when $Q_f = 70 \mu\text{l/min}$, L_f/D is only 3.5. This is because that when the flow rate of n-heptane is increased, evaporation of liquid fuel requires more heat, which decreases the wall temperature. When the wall temperature is below the boiling point of n-heptane, the interface constantly moves to the tube exit. Fig. 4 (b) shows that the wall temperature is decreasing with increasing of fuel flow rate. When $Q_f = 10 \mu\text{l/min}$, the maximum wall temperature could reach 1098K. But when $Q_f = 70 \mu\text{l/min}$, the maximum wall temperature is only 812K. It could be seen in Fig. 4(c) that there are two zone and three distinct boundaries. The first zone (Z1) is surrounded by a red frame and the second zone (Z2) is surrounded by a yellow frame. Three boundaries are the left boundary (B1) of Z2 and right boundary (B3) of Z1. B2 is the inter face between Z1 and Z2. Because there is a large part of black region in Z1 and the boundary B2 is semicircular, it can be deduced that Z1 is the three-dimensional interface between the gas and liquid n-heptane. The formation of the black region is attributed to that light emitted from a light source beneath the paper is refracted by the hemispherical two-phase interface. B3 is also the right boundary of fuel film on the tube wall due to wall dry-out. Furthermore, Z2 is a bubble observed from the side camera, which is attached on the top wall of the tube due to buoyance. And B1 is the left boundary of Z2.

3.2 Effects of fuel types on combustion characteristics

In order to understand effect of fuel type on micro diffusion flame, isooctane, ethanol, n-heptane and kerosene are used as liquid fuels and their combustion limits are obtained. The properties of four fuels are listed in Table 1.

Table 1 Properties of four fuels[2]

	N-heptane	iso-octane	kerosene	ethanol
Boiling point ($^{\circ}\text{C}$)	98.5	99.3	175-325	78.3
Combustion heat (J/kg)	48.07	47.67	43.1-46.2	29.71
Heat of vaporization (@ T_b , kJ/kg)	317	270	-	841
molecular formula	C_7H_{16}	C_8H_{18}	$\text{C}_{12}\text{H}_{26}$	$\text{C}_2\text{H}_5\text{OH}$
C/H mass ratio	5.25	5.33	5.54	4.00
Measured combustion limit($\mu\text{l/min}$)	5-70	5-50	5-50	35-100

Table 1 shows that the combustion heat of ethanol is the lowest in four fuels, which leads to its flammability limits different from other fuels. The first three fuels have the same lower combustion limit, i.e. $5 \mu\text{l/min}$, but that of ethanol is $35 \mu\text{l/min}$. It can be seen that heat of vaporization of ethanol is twice as large as that of other fuels. This indicates that evaporation of ethanol requires more heat when

the flow rate is the same for four fuels. Accordingly, the ethanol flame cannot be sustained at fuel flow rate lower than 30 $\mu\text{l}/\text{min}$. Except ethanol, other fuels had a stable flame when the flow rate was 5 $\mu\text{l}/\text{min}$.

It can also be seen in Table 1 that the upper limit of octane and kerosene is 50 $\mu\text{l}/\text{min}$, but that of n-heptane is 70 $\mu\text{l}/\text{min}$. This is because with increasing of fuel flow rate, liquid fuel in the micro tube cannot be completely evaporated, and there are some droplets with the fuel vapor ejected from the tube. Because combustion heat of n-heptane is the largest in four fuels, its upper limit is larger than that of octane and kerosene. Furthermore, Table 1 shows that the upper limit of ethanol is up to 100 $\mu\text{l}/\text{min}$ due to its largest evaporation heat in four fuels. This means that ethanol is not easy to evaporating, leading to ethanol film and suspension droplets formed on the tube wall. Therefore, the flame can be stable under large fuel flow rates.

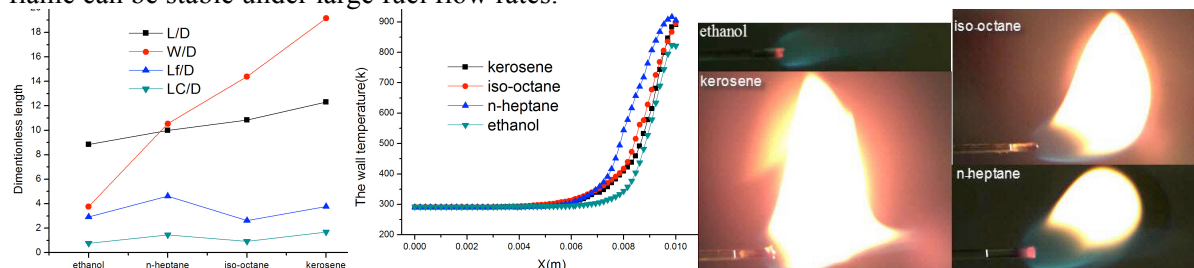


Fig. 5 Flame photos and combustion characteristics of fuels of four fuels at 40 $\mu\text{l}/\text{min}$. From left to right: (a) Flame size, (b) Wall temperature, (c) Flame photos

Fig. 5 (a) shows that with increasing of C/H, flame length L/D and flame width W/D increase monotonically. W/D of ethanol is the minimum and is only 2.9, while that of kerosene is the largest and up to 8.5. In Fig. 5 (b), we could see that the wall temperature gets increasing along the axis. Wall temperature of n-heptane is the highest and that of ethanol is the lowest. This is consistent with that when combustion heat of fuel is large, more heat is released by the fuel combustion, and hence the wall temperature is higher. In Fig. 5(c), we can see that there are great differences in four flames. Ethanol flame gives out weak blue light, while flame of other fuels emits bright yellow light. It may be attributed to different C/H ratios in four fuels. Table 1 shows that C/H of kerosene is the largest, followed by octane, and ethanol has the lowest C/H. Accordingly, ethanol flame has the blue light and no yellow light. Kerosene has the longest and brightest flame. Because C/H of n-heptane is larger than that of ethanol, there is blue light near the tube tip and bright yellow light at a position far from the tube in the n-heptane flame.

3.3 Effects of tube materials on combustion characteristics

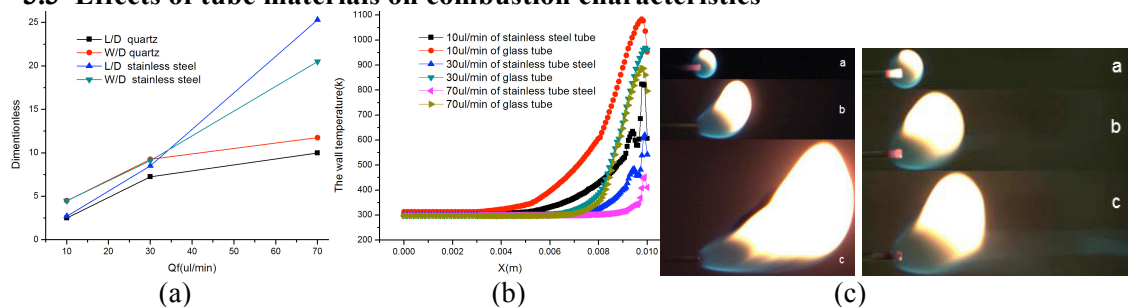


Fig. 6 Comparison of flames in SST and QT. (a) Flame length and width, (b) Wall temperature, (c) Flame photos, left: stainless steel tube; right: quartz tube. a: 10 $\mu\text{l}/\text{min}$, b: 30 $\mu\text{l}/\text{min}$, c: 70 $\mu\text{l}/\text{min}$

In order to study the effects of tube materials on flame characteristics, we used stainless steel tube (SST) and quartz tube (QT) with same size to supply liquid fuel. In the experiments, n-heptane is used and the flow rates are 10 $\mu\text{l}/\text{min}$, 30 $\mu\text{l}/\text{min}$ and 70 $\mu\text{l}/\text{min}$. Fig. 6(a) shows that the flame length and width of SST are larger than those of QT. When $Q_f < 30 \mu\text{l}/\text{min}$, the length and width of two flame are very close. While when $Q_f > 30 \mu\text{l}/\text{min}$, the flame length and width of SST increase significantly. These phenomena can also be seen in Fig. 6(c). When $Q_f = 10 \mu\text{l}/\text{min}$, two flame have the same size and shape.

But at $Q_f=70\mu\text{l}/\text{min}$, there is a great difference between two flame. The flame of SST is longer and wider than that of QT. And the former is brighter than the latter.

Fig. 6(b) indicates that wall temperature of QT is always higher than that of SST at the same fuel flow rate. When $Q_f=10\mu\text{l}/\text{min}$, the maximum wall temperature of QT is up to 1079K. While that of SST is only 836K. Furthermore, due to different wall temperature distributions, starting positions of n-heptane boiling are different. Since the boiling point of n-heptane is 371.7K, n-heptane in QT begins to boil at $X=0.0058\text{m}$, while in SST starts boiling at $X=0.0073\text{m}$. All of these is attributed to that thermal conductivity of SST is $15\text{W}/(\text{m}\cdot\text{K})$, 12.3 times larger than that of QT. Furthermore, as shown in left part of Fig. 6(c), when $Q_f>30\mu\text{l}/\text{min}$, the flame stays at a distance from the end of SST, and the end of SST is not heated red. But in right part of Fig. 6(c), the end of QT still is covered by the flame. Therefore, the quartz tube is heated to red.

In experiments, the maximum temperature of the micro stainless steel tube is no larger than 800°C , which occurs at the end of the tube. Temperature of other part of the tube is less than 650°C . To understand oxidization of the tube, the stainless steel tube is photographed by SEM after burning. It was found that different colours appear on the tube, as shown in Fig. 7. The position 1 is the exit, at which the flame is anchored. Between the positions 1 and 2, the tube wall is blue and the length is about 1mm. From the position 2 to 3, it appears dark brown. From the position 3 to 4, the wall colour changes gradually from dark brown to silver. Between the positions 4 and 6, there is now colour change.



Fig. 7 Photo of the micro stainless steel tube after burning

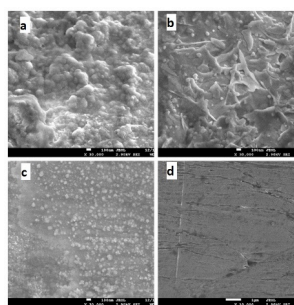


Fig. 8 SEM photos of the micro stainless steel tube at different positions. (a) position 1, (b) position 2, (c) position 3, (d) position 4.

Fig. 8 shows that there are oxidized layers at the positions 1 and 2. At the position 3, small oxide particles appear on the surface. But at the position 4, the surface is smooth, indicating no oxidization. It can be concluded that the oxidized part of the tube occurs at the region between 1 and 3. The distance between position 1 and 3 is about 2mm. Therefore, to ensure accurate measurement of the maximum temperature of the stainless steel tube, emissivity of the oxidized stainless steel is used in this study, which is 0.85.

Different thermal conductivity of SST and QT can lead to different evaporation modes in a micro tube. As shown in the literature[3], in a horizontal tube, with increasing of wall temperature, there are 5 different flow modes, i.e. single phase liquid flow, bubbly flow, slug flow, annular flow and single phase vapor flow. In this study, because wall temperature of SST is always lower than that of QT, the evaporation processes of liquid n-heptane in these two tubes are different. Fig. 6(b) shows that wall temperature gradient in SST is less than that in QT. When the n-heptane flow rate is small, such as $10\mu\text{l}/\text{min}$, the tube wall temperature is higher and the gas-liquid interface is far from the tube exit. Therefore, there are no droplets ejected from the tube exit. But in the case of higher n-heptane flow rate, the gas-liquid interface is near the tube end. At $Q_f=70\mu\text{l}/\text{min}$, the gas-liquid interface is only 3.5mm from the end of QT as shown in Fig. 4(a).

Fig. 6(b) shows that at $Q_f=70\mu\text{l}/\text{min}$, the position in SST, at which wall temperature is over 371.7K, is 0.5mm from the exit. But that in QT is 2mm from the exit and the maximum temperature in QT is up to 870K. Therefore, liquid fuel in SST appears annular flow, as shown in Fig. 9(b). In contrast, due to wall temperature over n-heptane boiling point, liquid fuel in QT appears dryout mist

flow, as shown in Fig. 9(c). Therefore, in Fig. 9(d), droplets are ejected from QT along the axis, forming a weak blue flame and the flame length of QT does not change greatly with fuel flow rate.

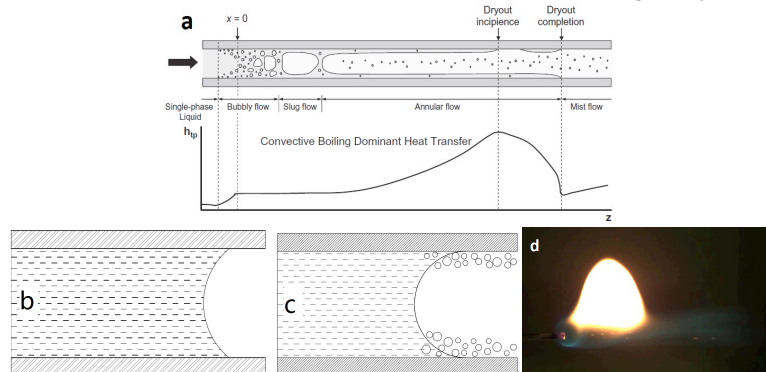


Fig. 9 Flow patterns during evaporation in a horizontal tube. (a) Schematics of flow regimes in reference [3], (b) annular flow in SST, (c) mist flow in QT, (d) photo of QT at 70 $\mu\text{l/min}$

4 Conclusions

Experimental studies were carried out to investigate micro diffusion combustion characteristics of liquid fuels from a micro tube. The following conclusions can be drawn:

- (1) Liquid fuel flow rate has great effects on flame length and shape. When n-heptane flow rate is lower than 10 $\mu\text{l/min}$, the flame is like a ball with a size less than 1mm, and the main reaction occurs at the tube exit. As the flow rate increases, flame length first increases and then is kept unchanged at $Q_f > 40 \mu\text{l/min}$. The gas-liquid interface moves toward the tube exit when Q_f is increasing.
- (2) Combustion heat, evaporation heat and C/H ratio of liquid fuels greatly influence the micro flame characteristics. Ethanol has the largest evaporation heat and the minimum combustion heat in four fuels. Its flame emits weak blue light and its lower combustion limit is higher than other fuels. But its flame can be sustained at a larger flow rate. Kerosene has the largest C/H ratio and hence its flame is the longest, emitting bright yellow light.
- (3) Thermal conductivity of the tube has a great influence on the flame. Flame length and width of the stainless steel tube are always larger than that of the quartz tube. But wall temperature of the former is lower than that of the latter. In the case of the quartz tube, at $Q_f > 40 \mu\text{l/min}$, small droplets are ejected from the tube due to boiling evaporation of n-heptane, generating a long blue plume along the tube axis at downstream the flame.

References

- [1] C.-P. Chen, Y.-C. Chao, T.S. Cheng, G.-B. Chen, C.-Y. Wu, Structure and stabilization mechanism of a microjet methane diffusion flame near extinction, *Proc. Combust. Inst.* 31 (2007) 3301–3308. doi:10.1016/j.proci.2006.08.069.
- [2] D.R. Lide, *CRC Handbook of Chemistry and Physics*, 85th Edition, CRC Press, 2004. http://books.google.co.uk/books/about/CRC_Handbook_of_Chemistry_and_Physics_85.html?id=WDI18hA006AC&pgis=1 (accessed December 22, 2014).
- [3] S.-M. Kim, I. Mudawar, Universal approach to predicting saturated flow boiling heat transfer in mini/micro-channels – Part I. Dryout incipience quality, *Int. J. Heat Mass Transf.* 64 (2013) 1226–1238. doi:10.1016/j.ijheatmasstransfer.2013.04.016.